Particle water and pH in the Eastern Mediterranean: Sources variability and implications for nutrients availability.

P. Nikolaou[1], A. Bougiatioti[1,2,*], I. Stavroulas[1], G. Kouvarakis[1], R. Weber[2], A. Nenes[2,3,4], M. Kanakidou[1], and N. Mihalopoulos[1,4,*]

1 Environmental Chemical Processes Laboratory, University of Crete, 71003 Crete, Greece
2 School of Earth and Atmospheric Sciences, Georgia Institute of Technology, Atlanta, GA 30332, USA
3 School of Chemical and Biomolecular Engineering, Georgia Institute of Technology, Atlanta, GA, 30332, USA
4 IERSD, National Observatory of Athens, Athens, GR-15236, Greece.

Keywords: aerosols, water content, pH, availability, nutrients

(*) Correspondence to: mihalo@uoc.gr ; kbougiatioti@gmail.com

Abstract

Particle water (LWC) and aerosol pH are important parameters of the aerosol phase, affecting heterogeneous chemistry and bioavailability of nutrients that profoundly impact cloud formation, atmospheric composition and atmospheric fluxes of nutrients to ecosystems. Few measurements of in-situ LWC and pH however exist in the published literature. Using concurrent measurements of aerosol chemical composition, cloud condensation nuclei activity and tandem light scattering coefficients, the particle water mass concentrations associated with the aerosol inorganic (W_{inorg}) and organic (W_{org}) components are determined for measurements conducted at the Finokalia atmospheric observation station in the eastern Mediterranean between August and November 2012. These data are interpreted using the ISORROPIA-II thermodynamic model to predict pH of aerosols originating from the various sources that influence air quality in the region. On average, closure between predicted aerosol water and that determined by comparison of ambient with dry light scattering coefficients was achieved to within 8% (slope=0.92, R^2=0.8, n=5201 points). Based on the scattering measurements a parameterization is also derived, capable of reproducing

the hygroscopic growth factor (*f(RH)*) within 15% of the measured values. The highest aerosol water concentrations are observed during nighttime, when relative humidity is highest and the collapse of the boundary layer increases the aerosol concentration. A significant diurnal variability is found for W_{org} with morning and afternoon average mass concentrations being 10-15 times lower than nighttime concentrations, thus rendering W_{inorg} the main form of particle water during daytime. The average value of total aerosol water was 2.19±1.75 μg m^{-3}, contributing on average up to 33% of the total submicron mass concentration. Average aerosol water associated with organics, W_{org}, was equal to 0.56±0.37 μg m^{-3}, thus organics contributed about 27.5% to the total aerosol water, mostly during early morning, late evening and nighttime hours.

The aerosol was found to be highly acidic with calculated aerosol pH varying from 0.5 to 2.8 throughout the study period. Biomass burning aerosol presented the highest values of pH in the submicron fraction and the lowest values in total water mass concentration. The low pH values observed in the submicron mode and independently of air masses origin could increase nutrient availability and especially P solubility, which is the nutrient limiting sea water productivity of the eastern Mediterranean.

1. Introduction

Atmospheric particles have the ability to absorb significant amounts of water, which profoundly affects their physical and chemical properties (Khlystov et al., 2005), and impacts on atmospheric processes and health. Ambient concentrations of aerosol liquid water are controlled by the aerosol chemical composition, relative humidity (RH) and temperature, as it is largely in chemical equilibrium with the surrounding water vapor. Liquid water is ubiquitous and exceeds the total aerosol dry mass by 2 to 3 times on a global scale (Liao and Seinfeld, 2005). Therefore, the aerosol liquid water content (LWC) increases the particle size, affecting the particle lifetime and scattering efficiency. LWC and its strong dependence on relative humidity (RH) are the most important contributors to aerosol direct radiative cooling by aerosols (Pilinis et al., 1995). Numerous modeling studies suggest that reactions in aerosol liquid water are an important pathway of secondary organic aerosol (SOA) formation (Carlton and Turpin, 2013; Myriokefalitakis et al., 2011), thus playing an important role in the overall aerosol chemical composition. Aerosol water also has profound impact on the aerosol phase state, being able to transform semi-solid and viscous

particles into homogeneous phase that are in equilibrium with their environment (Pöschl and Shiraiwa, 2015). This affects the timescale of heterogeneous reactions and ice nucleation. Nevertheless, despite the abundance and importance of LWC, it is not routinely measured, actual mass concentrations are uncertain, especially in the presence of organic compounds and model predictions of the property are often not evaluated (Nguyen et al., 2014).

Apart from the LWC, the pH of aqueous aerosols is another critically important aerosol property that drives many processes related to the aerosol chemical composition and gas-aerosol partitioning (Guo et al., 2015; Surratt et al., 2007; 2010; Meskhidze et al., 2003; Eddingsaas et al., 2010; Myriokefalitakis et al., 2015). Direct measurements of aerosol pH "in situ" are scarce (e.g., Keene et al., 2002; 2004) and require careful considerations owing to the non-conserved nature of the hydronium ion and partial dissociation of inorganic and organic electrolytes in the aerosol. These challenges have led to the suggestion that indirect alternatives – such as measuring the semi-volatile partitioning of key species sensitive to pH, combined with comprehensive models may provide a reasonably accurate estimate of pH that can be carried out with routine measurements (Hennigan et al., 2015). The most frequently used proxy is the "ion balance", where the charge balance of measurable anions and cations is calculated, with the exception of the hydronium and hydroxyl ions; a surplus of cations implies an alkaline aerosol and vice versa. Often it is implied that a larger value of the ion balance implies a stronger acidity/alkalinity. As shown by Hennigan et al. (2015) and Guo et al. (2015), the ion balance (and other similar proxies discussed in Hennigan et al., 2015) fail in general to represent the true aerosol pH; only meticulous measurement of semi-volatile species (such as ammonia/ammonium) and other aerosol chemical constituents, combined with appropriate thermodynamic calculations (e.g. with ISORROPIA-II; Fountoukis and Nenes, 2007) are able to realistically provide particle pH and LWC (Hennigan et al., 2015). For an accurate and unbiased pH calculation both gas and aerosol phase concentrations are needed, however, when some uncertainty can be tolerated or the level of pH bias is known, aerosol measurements alone can still be quite informative for determining the pH, as demonstrated by Guo et al. (2015).

Directly linked to aerosol pH and LWC is the bioavailability of nutrients contained within dust, involving pH-dependent catalyzed redox-reaction pathways; upon deposition, increased availability of these nutrients may promote primary productivity in continental and marine ecosystems (e.g., Meskhidze et al., 2003; Nenes et al., 2011; Mahowald et al., 2008; 2009;

Krishnamurthy et al., 2010). Acids (such as sulfuric and nitric) generated in the atmosphere from a variety of anthropogenic and biogenic sources, when mixed with mineral aerosols in sufficient amounts could lower the aerosol pH to values that increase the solubilities of Fe and P-containing minerals by several orders of magnitude (Stumm and Morgan, 1996; Shi et al., 2012). Nenes et al. (2011) have demonstrated that acidification can release considerable amounts of soluble phosphorus from soil-laden minerals (e.g., 81-96% of the total P found in Saharan dust and soil). Apart from P, the transport and deposition of mineral dust is believed to be a major, if not the dominant source of Fe to the remote ocean (Jickells et al., 2005). Considering the mixing of SO_2 with advected dust plumesand the subsequent acidification through heterogeneous oxidation of the SO_2 on deliquescent dust particles within the plume, , Meskhidze et al. (2003) concluded that for aerosol with pH <2, 1-2% of the contained Fe would be mobilized within 3-5 days. Meskhidze et al., (2005) also demonstrated that sufficient acidification of Asian dust plumes could drive, upon deposition, a phytoplankton bloom in High Nitrate Low Chlorophyll regions of the North Atlantic. Solmon et al. (2009) also showed that simulated enhancements in particulate soluble iron driven by the chemical dissolution mechanism, can range from 0.5 to 6%, which is consistent with observations over the North Pacific Ocean.

The Eastern Mediterranean, being at the nexus of three continents (Europe, Asia and Africa), receives air masses influenced by a spectrum of human (traffic, biomass burning and industry) and natural (dust and marine) sources. It is therefore an ideal location to study atmospheric acidification of aerosols; very few studies however to date have accomplished that.

This study uses aerosol chemical composition measurements in conjunction with cloud condensation nuclei (CCN) concentration and light scattering coefficient (σ_{sp}) measurements to model the water mass concentrations (LWC) of aerosols from various sources in the Eastern Mediterranean. These data are then used in combination with the ISORROPIA-II thermodynamic equilibrium model (Fountoukis and Nenes, 2007) to predict the aerosol pH for air masses that influenced air quality in the Eastern Mediterranean during the late summer and fall months of 2012.

2. Instrumentation and Methods

2.1 Measurement site

Aerosol measurements were conducted at the Finokalia atmospheric observation station in Crete, Greece (35°20'N, 25°40'E, 250m a.s.l.) between August and November 2012. The site (http://finokalia.chemistry.uoc.gr/) is a European supersite for atmospheric aerosol research and is part of the ACTRIS Network (Aerosols, Clouds, and Trace gases Research Infrastructure) (http://www.actris.eu/). The station is located at the northeastern part of the island of Crete, facing the Mediterranean Sea covering the whole northern sector. Being away from direct urban influence, the station is representative for background measurements in the Eastern Mediterranean and sampled air masses arriving at the site have most commonly a marine source region or originate from continental Europe and Greek mainland. Moreover, dust events from Northern Africa (Sahara) occur often during spring and autumn. More details for the Finokalia station and the prevailing climatology in the area are given by Mihalopoulos et al. (1997).

2.2 Instrumentation

PM_1 (Particulate Matter of diameter smaller than 1 μm) aerosol light scattering coefficients (σ_{sp}) were measured online with the use of two different nephelometers to infer the LWC. Particle dry scattering was measured with a 3-wavelength Aurora 1000 Integrating Nephelometer, located in an air-conditioned sampling trailer and operated with a diffusional silica dryer upstream, which maintained the RH below 35%. Based on the ISORROPIA model run for metastable ammonium sulfate aerosol at an RH of 30%, the maximum water which can be contained under these conditions is 1.21 μg m^{-3}, which is less than 12% of the total submicron aerosol mass. The nephelometer for the particle wet scattering was a Radiance Research M903, located outside the trailer in order to provide a scattering measurement at ambient T and RH. This second nephelometer was equipped with a VAISALA Inc. Humitter 50U Integrated Humidity and Temperature probe in order to record the ambient values of T and RH with an accuracy at 20 °C specified to be better than ±5% RH . Both nephelometers take part in yearly intercomparisons within the ACTRIS network.

The real-time, quantitative measurements of the non-refractory components of the submicron aerosol were provided by an Aerosol Research Inc. Aerosol Chemical Speciation Monitor (ACSM; Ng et al., 2011). Ambient air was draw into the ACSM by a multiple PM_{10} (Particulate Matter of diameter smaller than 10 μm) aerosol inlet operating at Finokalia, with a temporal resolution of 30

minutes. At the inlet of the ACSM and via a critical aperture mounted at the entrance of an aerodynamic lens, the submicron fraction of the aerosol is sampled. The aerodynamic lens of the ACSM allows for the detection of particles up to 700 nm diameter. The focused particle beam is then transmitted through two vacuum chambers and into a detection chamber where the particles impact on a hot plate and flash vaporized. Finally they are detected and characterized with the use of an electron impact quadrupole mass spectrometer. Constituents quantified by the ACSM include organics, sulfate, ammonium, nitrate and chloride. Detection limits for all constituents for 30 min of averaging time are provided by Ng et al. (2011) and are for ammonium, organics, sulfate, nitrate, and chloride are 0.284 μg m^{-3}, 0.148 μg m^{-3}, 0.024 μg m^{-3}, 0.012 μg m^{-3}, and 0.011 μg m^{-3}, respectively. Mass concentrations are calculated with the recommended collection efficiency of 0.5 for all constituents (Ng et al. 2011) and the main aerosol constituents i.e. organics, sulfate and ammonium are verified by comparison with other concurrent measurements (daily PM_1 filters; Bougiatioti et al. (2014) supplementary material). PM_1 filters (Pallflex Tissuquartz, 47 mm diameter) were collected using a built-in system comprised of the four upper stages (stage 8-11) of a low-pressure Berner impactor (PLBI; Berner and Lürzer, 1980). Furthermore, daily PM_{10} filters are also collected on site using a sequential sampler (Leckel, SEQ47/50). A detailed study of the comparison between ACSM and PM_1 filter values for a large subset of the present data (16/08-30/09/2012) is provided by Bougiatioti et al. (2014).

PM_1 and PM_{10} filters were analyzed by ion chromatography (IC) for anions (Cl^-, Br^-, NO_3^- (nitrate), SO_4^{-2} (sulfate), $C_2O_4^{-2}$ (oxalate)) and cations (K^+, Na^+, NH_4^+ , Mg^{2+}, Ca^{2+}) using the procedure described by Bardouki et al. (2003). From the calcium, the crustal component can be estimated by subtracting the contribution of sea-salt Ca^{2+} = [Na]*0.038 and dust concentration is estimated using the approach of Sciare et al. (2005). Based on the study by Koulouri et al. (2008) for a two-year period at the same sampling site, it has been demonstrated that for fine particles (in that case D_a<1.3 μm) the contribution of the marine source to the aerosol mass was 10%. Similarly, dust contribution in the fine fraction can vary between 6 and 10% for summer and winter, respectively.

From 25/6 to 7/8/2014, gas phase ammonia measurements were also conducted at Finokalia, using a wet annular denuder (WAD; Wyers et al., 1993; Spindler et al., 2003) coupled with an ion chromatography system quantifying cations with an hourly resolution in order to check the validity of our calculations in the absence of gaseous phase NH_3 (see section 2.4). Concurrent black carbon

(BC) measurements were performed on site using a seven-wavelength aethalometer (Magee Scientific, AE31) with a time resolution of 5 min. Based on previous studies at Finokalia, BC is found mainly on the fine aerosol fraction (Koulouri et al., 2008; Bougiatioti et al., 2014) hence these values are used in addition to the ACSM concentrations to calculate the dry aerosol mass of the PM_1 fraction.

Size-selected cloud condensation nuclei (CCN) measurements were obtained using a Droplet Measurement Technologies, Continuous Flow Streamwise Thermal Gradient CCN counter (CFSTGC). Particles of 60, 80, 100 and 120 nm were first size-selected by a differential mobility analyzer (DMA), split into two and one of these flows was introduced in the CCN counter. The total number of condensation nuclei (CN) was measured by a condensation particle counter (CPC; TSI 1772) situated downstream the first DMA. In the CCN counter, the activated droplets are sized and counted by an optical particle counter (OPC) after exiting the growth chamber. The instrument was operated in scanning flow CCN analysis mode (SFCA; Moore and Nenes, 2009), where the flow rate in the growth chamber changes over time, while a constant temperature difference is maintained. In that way the supersaturation changes continuously, providing activation spectra with a high temporal resolution. The flow rate was increased linearly between a minimum and a maximum flow rate and sigmoidal activation curves of CCN vs flow rate were recorded, with the inflection point of the sigmoid representing a critical activation flow, Q_{50}, that corresponds to a critical supersaturation, S^*, above which particles act as CCN. From the critical supersaturation and knowledge of the particle dry diameter, with the application of Köhler theory, the hygroscopicity parameter kappa (Petters and Kreidenweis, 2007) is obtained, which is then used to determine the LWC associated with organic components of the aerosol (Guo et al., 2015).

Finally, analysis of 5-day back trajectories of air masses arriving at Finokalia at 1000 and 3000 m above ground level every 6 h was conducted with the help of the HYSPLIT model (www.arl.noaa.gov /hysplit.php; Stein et al., 2015).

2.3 Determination of LWC from nephelometers

The particle water was inferred using the approach of Guo et al. (2015), where the ratio of the wet and dry PM_1 scattering coefficients (σ_{sp}) measured by the two nephelometers is used. For this, the aerosol hygroscopic growth factor ($f(RH)$) is calculated according to a well-established method based on the two scattering coefficients: $f(RH)=\sigma_{sp(wet)} / \sigma_{sp(dry)}$ (e.g. Sheridan, 2002; Magi, 2003;

Kim et al., 2006). These scattering coefficients in ambient and dry conditions are proportional to the diameter of average surface $\overline{D_p}$ and the average scattering coefficients $\overline{Q_s}$, so that :

$$\overline{D_{p,ambient}} = \overline{D_{p,dry}} \sqrt{f(RH)\overline{Q_{s,dry}} / \overline{Q_{s,ambient}}} \qquad (1)$$

Assuming that the two average scattering efficiencies are almost equal, LWC is then equal to the difference between ambient and dry particle volume, and by substitution of the dry diameter of average surface:

$$\overline{D_{p,dry}}^3 = \frac{m_p}{\left(\frac{\pi}{6}\right)\rho_p N_t} \qquad (2)$$

where N_t is the total number concentration, ρ_p is the density of dry aerosol and m_p is the dry mass concentration, we arrive at the simplified expression of:

$$LWC = [f(RH)^{1.5} - 1]\frac{m}{\rho_p} \qquad (3)$$

The simplification assumption that the dry and ambient scattering efficiencies are almost equal introduces an error in the derived LWC, which based on the detailed analysis of Guo et al. (2015) is of the order of 10% at RH=76.4%, but can reach up to 21% at RH=90%.

For this set of measurements the PM_1 dry mass concentration is calculated from the sum of the ACSM constituents combined with the BC measurements. During the sampling period, the comparison between the sum of ACSM and BC masses and the submicron mass derived from a scanning mobility particle sizer (SMPS; TROPOS-type) is very good (y=0.96x, R^2=0.67 for a period of 2-years; Figure S3). Therefore the bias introduced by ignoring other refractory constituents than BC is minimal, which is in agreement with size-segregated aerosol chemical composition measurements already conducted at Finokalia (e.g. Koulouri et al., 2008). The particle density, ρ_p, was estimated from the particle composition from the ACSM ammonium, organics and sulfate, using an organic density of 1.35 g cm^{-3} as determined by Lee et al. (2010) for the same site during the summer of 2008, the density of ammonium sulfate (1.77 g cm^{-3}) and the equation:

$$\rho_p = \left[\frac{x_{a/s}}{\rho_{a/s}} + \frac{x_{org}}{\rho_{org}}\right]^{-1} \qquad (4)$$

where $x_{a/s}$ is the mass fraction of ammonium sulfate and x_{org} is the mass fraction of the organics, and $\rho_{a/s}$ and ρ_{org} are the densities of ammonium sulfate and the organics, respectively. It must be

noted that nitrate is not taken into account as its concentrations are very close to the limit of detection of the ACSM for the PM_1 fraction at the Finokalia site during the studied period. Particle density was calculated to be 1.56±0.08 g cm^{-3} (n=6028), with aerosol concentration ranging from 1.33 to 16.65 μg m^{-3} and average value of 5.62±3 μg m^{-3}. The particle water calculated by this method is hereafter referred to as *f(RH)*_water, with the uncertainty of this calculation being estimated to be 23% (Guo et al., 2015).

2.4 LWC and pH prediction from chemical composition

The water vapor uptake by aerosol establishing equilibrium for ambient temperature and relative humidity conditions is influenced by both inorganic and organic components. LWC, therefore, is directly dependent on aerosol chemical composition and meteorological conditions, as well. As proposed by Guo et al. (2015) and explained below, we calculated the particle water associated with inorganics (W_{inorg}) and the particle water associated with organics (W_{org}). The sum of these two ($W_{inorg}+W_{org}$), equal to the total particle water, is then compared to the LWC determined by the two nephelometers.

First the particle pH was calculated by the thermodynamic model ISORROPIA-II for the PM_1 aerosol fraction. W_{inorg} was calculated based on a thermodynamic equilibrium between an inorganic aerosol (NH_4-SO_4-NO_3-Cl-Na-Ca-K-Mg-water) and its gas phase precursors. For the current analysis, the inputs to ISORROPIA-II are the inorganic ions measured by the ACSM with a 30 min time resolution (except for Cl which is at the detection limit of the instrument at the specific site), the average daily values for Na^+, Cl^-, Ca^{2+}, K^+ and Mg^{2+} determined by ion chromatography analysis of PM_1 filters, and RH and T measured by the ambient nephelometer probe. The use of daily values for the macromineral elements obtained from the filter analysis could introduce potential artifacts in the calculation, but is believed to be limited as almost 90% of the fine fraction mass in the area can be attributed to ammonium sulfate and organics (Koulouri et al., 2008; Bougiatioti et al., 2009;2013).

The contribution of the organic components to particle water (W_{org}) was determined from the organic hygroscopicity parameter (κ_{org}) from the observed CCN activities of the organic fraction (Cerully et al., 2014):

$$W_{org} = \frac{m_s}{\rho_s} \frac{\kappa_{org}}{\left(\frac{1}{RH} - 1\right)} \qquad (5)$$

where m_s and ρ_s are the organic mass concentration from the ACSM and an organic density, respectively determined as described in section 2.3.

Finally, the particle pH is calculated by the thermodynamic model ISORROPIA-II (Fountoukis and Nenes, 2007) based on the calculated equilibrium particle hydronium ion concentration in the aerosol. As ISORROPIA-II does not take into account the LWC associated with the organic aerosol, a recalculation of pH is made by considering the predicted particle hydronium ion concentration per volume of air (H^+_{air}) and the total predicted water ($W_{inorg}+W_{org}$) (Guo et al., 2015):

$$pH = -\log_{10} H^+_{aq} = -\log \frac{1000 H^+_{air}}{W_{inorg} + W_{org}} \qquad (6)$$

where the modeled concentrations for LWC and H^+_{air} are μg m^{-3}, and H^+_{aq} (mol L^{-1}) is the hydronium concentration in an aqueous solution and W_{inorg} and W_{org} are in μg m^{-3}. ISORROPIA-II has been previously tested and was able to predict the equilibrium partitioning of ammonia and nitric acid to within measurement uncertainty (Nowak et al., 2006; Fountoukis et al., 2009; Hennigan et al., 2015; Guo et al., 2015). Here, ISORROPIA-II was run in the "forward mode" assuming a metastable aerosol state. It should be noted that gas phase measurements of ammonia ($NH_{3(g)}$) were generally not available for the whole measurement period and the sum of NH_3 and NH_4^+ is assumed to be equal to NH_4^+. Therefore it is expected that the pH could be underpredicted by at most one unit (Guo et al., 2015; Weber et al., 2016).

To assess the uncertainty in our calculations by not including gas phase NH_3, a sensitivity analysis is performed by adding different amounts of $NH_{3(g)}$ to the system and quantifying the response in pH. Initial results of ISORROPIA, were compared to results obtained after adding 0.5, 1.2, 3.2 and 5 μg m^{-3} of ammonia. The values of 1.2 and 3.2 μg m^{-3} were the median and maximum values of the gas phase measurements conducted with the WAD during summer 2014, respectively. These values are also within the observed values reported by Guo et al. (2015). A 3-year study conducted at the Finokalia station (Kouvarakis et al., 2001) reported that $NH_{3(g)}$ concentrations during summertime have an average of 0.27 μg m^{-3} (range from 0.07 to 0.68 μg m^{-3}). Thus, a lower value (0.5 μg m^{-3}) to represent these measurements was also applied and finally 5 μg m^{-3} was selected

as an extreme value which is very close to the European critical level for NH_3, established to 8 μg m^{-3} as an annual mean (Air Quality Guidelines for Europe, 2000). The results of the sensitivity study are provided in detail in the supplementary material and clearly show that neglecting the gas phase NH_3 in the calculations leads to an underestimate of around 0.5 units in the pH (from 1.38 to 1.85 median values) for the NH_3 range reported for Finokalia.

The above results are further supported by the partitioning of nitric acid between the condensed (NO_3^-) and gas phase (HNO_3). Assuming ideal solutions for the average conditions during the study period derived from ISORROPIA-II, it is calculated that little nitrate should be present in the aerosol phase when pH is lower than 3 (Figure S5 Supplementary). Indeed, with an average concentration of nitrates of 0.12±0.06 μg m^{-3} in the fine mode and the resulting partitioning coefficient of less than 0.2, it is derived that the maximum value of pH that can be observed for the current conditions is 2. This value is in total accordance with the upper limit of pH of 1.85 derived from the formerly presented sensitivity analysis.

For days where $NH_{3(g)}$ measurements exist (summer 2014), following the same methodology as before, the measured concentrations of $NH_{3(g)}$ and predictions by the model are in fairly good agreement. Observed gas phase concentrations have an of 0.79±0.27 μg m^{-3} while predicted concentrations have an average of 0.65±0.32 μg m^{-3}. Additionally, we directly compared the pH and LWC values derived from ISORROPIA in the forward mode when calculations were initiated with total (NH_3+NH_4^+) versus paired results (n=328) for the respective ones initiated with only particulate phase NH_4^+. The results show that for the specific periods, the addition of NH_3 in the calculations has a minor effect to both pH (y=0.965x, R^2=0.584) and LWC (y=1.055x, R^2=0.993).

3. Results and Discussion

3.1 PM_1 chemical composition and f(RH)_water

For the measurement period, the average values for the main aerosol constituents were 1.85±0.94, 2.31±1.61, 0.81±0.58 and 0.52±0.22 μg m^{-3} for organics, sulfate, ammonium and BC, respectively. In terms of contribution to the PM_1 mass concentration, the two most abundant components of the submicron range were sulfate and organics, with mass fractions of 39.6 and 33.8% respectively, followed by ammonium (14.8%), BC (9.3%) and nitrate (2.1%). Chloride has a negligible contribution to the total submicron mass concentration. The time series of the main aerosol

constituents and their overall contribution, as measured by the ACSM, are portrayed in Figure 1. Nevertheless, a fluctuation of 10-20% in sulfate and/or ammonium concentrations is not expected to be reflected in a pH change, given the logarithmic scale of the property, which is consistent with the findings of Weber et al. (2016) that pH has a weak sensitivity to a wide range of SO_4^{2-} and NH_3. This is further elaborated by the sensitivity analysis of gas phase ammonia, where the 5-fold increase of added amount of NH_3 causes a unit change in pH, on average. More details about the ACSM measurements and performance can be found in Stavroulas et al. (in preparation, 2016).

The chemical composition is expected to influence the water content of aerosol, as well. Mean *RH* and *T* during the study period were 57±11% and 27.4±3.7 ºC. As described in the section 2.3, *f(RH)*_water was calculated from the data from the two nephelometers. With the use of equations 1 and 2, we calculated LWC from the nephelometers for the whole measurement period. The average value of *f(RH)*_water was 2.19±1.75 μg m^{-3}, which according to the dry mass measurements, can contribute on average, up to 33% of the total submicron mass concentration. We also sought to establish a link between *f(RH)* and *RH* and taking into account all available scattering data (n=7044) the following parameterization has been established:

$$f(RH) = 1.067(\pm 0.004) + 1.99(\pm 1.05) \cdot 10^{-7} RH^{3.547(\pm 0.035)} \qquad (7)$$

Based on this, we reconstructed the time series of the hygroscopic growth factors, with a very good correlation between calculated and measured values (y=0.99x, R^2=0.85) (also see Supplementary Material). This parameterization does not appear to be influenced by changes in the chemical composition. Uncertainties in the RH measurement by the probe are in the order of 5% while dry and wet aerosol light scattering coefficients measurement uncertainty is in the order of 20%.

3.2 Inorganic and organic water predictions

3.2.1 Inorganic aerosol water

The thermodynamic model ISORROPIA-II (http://isorropia.eas.gatech.edu; Fountoukis and Nenes, 2007) was used to predict the contribution of inorganic species to LWC. The water attributed to the inorganic component of the aerosol has an average value of 1.77±1.45 μg m^{-3}. The lowest values are observed during August, probably because of the higher temperatures that enhance evaporation of water from the aerosol. The timeseries for aerosol water associated both with inorganic and organic aerosol components are shown in Figure 2, where it can be seen that most of the time, the variability of the two water components follow each other closely, with water

concentrations associated with organics being about 1:10 (12±9%) of those associated with the inorganic aerosol components.

3.2.2 Organics: hygroscopicity and aerosol water

The contribution of the organic submicron fraction of the aerosol to the particle water was calculated from the combination of the CCN and chemical composition measurements, as described in section 2.4. Assuming that the cumulative aerosol hygroscopicity can be represented as the sum of contribution of the inorganic (expressed mostly by ammonium sulfate) and organic fraction of the aerosol, the measured hygroscopicity can be calculated by the sum:

$$\kappa = \varepsilon_{inorg}\kappa_{inorg} + \varepsilon_{org}\kappa_{org} \qquad (8)$$

where ε_j and κ_j are the volume fraction and hygroscopicity of the inorganic and organic species. Once the aerosol species concentrations are determined, the corresponding volume fractions for ammonium sulfate and organics are calculated, and a set of hygroscopicity parameter equations is produced. As mentioned in the section 2.2, hygroscopicity parameters for 60, 80, 100 and 120 nm particles are measured. In a former CCN study at the same site (Bougiatioti et al., 2011) it was shown that from many different particle sizes, the characteristic hygroscopicity parameter κ^* of the 100 nm particles was the closest one to the κ determined by PM_1 filter measurements. Therefore we created two different sets of kappa equations along with the volume fractions to calculate the total κ^*, one for the 100 and another one for the 120 nm. With the subsequent application of multivariate regression analysis to the set of n=2429 and 1801 equations (for 100 and 120 nm respectively), κ_{org} is determined to be 0.28±0.01 based on the $\kappa_{\_100nm}$ and 0.24±0.01 based on the $\kappa_{\_120nm}$. The average value of 0.26 is used in equation 5 to calculate the time series of W_{org}. The average value W_{org} was thus found to be 0.56±0.37 μg m^{-3}, which constitutes on average ~27.5% of the calculated *f(RH)*_water. The overall uncertainty of this calculation is estimated by Guo et al. (2015) to be around 30%. That study for south eastern United States of America, found a higher contribution of organic species (on average 35%) to the total water that can be explained by the dominance of organics in the submicron range aerosol, with an average mass fraction of 67%.

3.2.3. Aerosol water

Aerosol water is the sum of W_{org}+W_{inorg}, determined as previously explained. This can be further compared with the time series of the *f(RH)*_water deduced from concurrent observations by the

two nephelometers (section 2.3), independent from the aerosol water calculated as here explained. The particle water predicted from the sum of the organic and inorganic contributions to the water agrees very well with the water measured by the nephelometers (Figure 3). More specifically, the total predicted water is highly correlated and on average within 10% of the measured water, with slope=0.92 and R^2=0.8 for the whole measurement period (n=5201 points).

The diurnal variability of the calculated water components, along with the total measured water, ambient T and RH is shown in Figure 4. It must be noted at this point that the presented diurnal variability corresponds to the entire period of the study and this pattern seems to be independent of the geographical sector and/or source region, based on the backtrajectory analysis. The diurnal variability of aerosols from different sources, further presented at Section 3.4, have been explicitly studied and found not to differ significantly, therefore the total diurnal variability was selected as being representative of the whole measurement period. Predicted and measured aerosol LWC diurnal variabilities are in very good agreement. As expected, the highest LWC values are observed during nighttime, when RH is also at its maximum, resulting in significant water uptake. W_{org} shows a significant diurnal variability with morning and afternoon average mass concentrations being 10-15 times lower than nighttime ones. Thus, during daytime W_{inorg} is the main component of particle water as the average values for the predicted water (W_{org}+W_{inorg}) are very close to the ones of the inorganic water alone. On the other hand, during nighttime, the two averages start to diverge and this could be attributed to the higher contribution of organic water during nighttime, when the photochemical activity and temperature are minimum and RH high.

3.3 Aerosol pH

The predicted pH for the aerosols collected at Finokalia during the studied period was highly acidic with an average value of 1.25±1.14 (median 1.51) and varying between -0.97 and 3.75. pH varied by almost 1 unit throughout the day. This can be translated as an almost 10-fold increase of the H^+_{air}/LWC ratio from early morning to mid-day and to a lesser extent during early night. This significant variation in pH can be partially explained by the diurnal variation of H^+ and its increase which coincides temporally with the decrease in pH (Figure 5) and by the reduction of aerosol water (LWC) during daytime compared to the higher LWC during nighttime (Figure 4). This implies the diurnal variability of pH is mostly driven by the reduction of aerosol water during daytime compared to the higher aerosol water during nighttime.

When studying the diurnal variability of pH for the different sources/geographical sectors (supplementary material) it occurs that pH differs depending on the source and origin of the air masses. Air masses from the northwestern, northeastern Europe and Turkey, as well as from Greek mainland, do not exhibit significant diurnal variability. When no distinction is made between source regions, the pattern of the overall pH variability with a drop in pH values during midday as presented in Fig. 5, is similar to the diurnal variability of pH for air masses influenced by mineral dust (coming from the SW) and by biomass burning, but with pH values from biomass burning being 1-1.5 units higher. Nevertheless, the mean pH values for each one of the source regions are very close to the overall pH mean value when no distinction of origin is made.

Furthermore, accounting only for the water associated with the inorganic aerosol component, particle water is underestimated by around 9%, thus resulting in a slightly lower pH (more acidic) by 0.07-0.38 units of pH (Figure 6a). As seen in section 3.2, W_{org} is on average 27.5% of the total water, as a result the pH increases by 0.14 units when the organic water is included (Figure 6a). When the contribution of organic water is taken into account, the recalculation of pH gives an average value of 1.38±1.11 (median 1.65). The pH calculated by ISORROPIA-II correlates very well with the pH corrected using equation 6 for inclusion of the organic water (W_{org}+W_{inorg}) (R^2=0.98, Figure 6b). Subsequently, if organic mass and organic hygroscopicity data are not available, ISORROPIA-II solely based on inorganic composition data, will provide an adequate estimate of both H^+_{air} and W_{inorg} and thus of pH.

3.4 Aerosol water and pH based on aerosol fraction and source region

Apart from the time-resolved aerosol water and pH calculations for the submicron aerosol fraction, aerosol water and pH were also calculated based on the daily PM_{10} filter chemical composition analysis. It should be noted at this point that there is a strong link between aerosol pH and aerosol size distribution due to the chemical composition changes in the aerosol size. For PM_1 which is in equilibrium and chemical composition is determined by high time resolution measurements leads to higher accuracy in the pH calculations. On the other hand, as PM_{10} particles are not in equilibrium, the respective acidity results are subject to biases and are less quantitative than the submicron results. For comparison purposes the corresponding PM_1 measurements, based on ACSM and the respective PM_1 ionic concentrations for cations such as Na^+, Ca^{2+}, Mg^{2+}, corresponding to the fine fraction, have also been averaged to daily values. Characteristic source regions/sources

were subsequently selected based on back-trajectory analysis and chemical tracers. Furthermore, biomass burning events have been identified based on source apportionment of BC and Positive Matrix Factorization (PMF) analysis of the organic mass spectra obtained from the ACSM as detailed in Bougiatioti et al. (2014). Dust events were identified by backtrajectory analysis of the air masses, originating from Northwestern Africa and confirmed as by containing large amounts of particulate matter (45-55 μg m^{-3} in PM_{10} mass) and high concentrations of crustal ions, such as Ca^{2+} (median concentration during dust events of 1.8 μg m^{-3} versus 0.6 μg m^{-3} for the rest of the days) . The main measured and calculated parameters are presented in Table 1.

It can be seen that, in general, for anthropogenic-laden air masses (e.g. from Istanbul, Black Sea and Continental Europe) aerosol mass resides mainly (60-70%) in the submicron aerosol and thus the submicron fraction seems also to drive the pH of PM_{10}, while most of the aerosol water (~70%) is present in the coarse fraction. Biomass burning exhibits the highest values of pH in the submicron fraction and the lowest values in total water mass concentration. Interestingly enough, the value of 2.77 for biomass burning pH is well above the value of 2, which favors the partitioning of nitrate to the aerosol phase (e.g., Meskhidze et al., 2003) The correlation observed during fire events between biomass burning organic aerosol and particulate nitrates (e.g. Bougiatioti et al., 2014) may be explained by these higher pH levels, rather than just high levels of nitric acid and/or ammonia. As found in the literature, higher pH levels of biomass burning aerosol can also be attributed to higher concentrations of non-sea salt potassium, which as an ionic species influences pH (Zhang et al. 2015), rendering aerosol more alkaline. Based on the calculated ratios for pH and particle water, it can be derived that the ions that set the bulk pH is mostly driven by the fine mode; the LWC however is associated mostly with the supermicron aerosol mass. Hygroscopic sea salt components are also found in the coarse mode, which can justify the larger contribution of PM_{10} total water, while the submicron fraction may be composed mostly of less hygroscopic, organic components (Bougiatioti et al., 2015). Even though strong dust events were lacking during the study period, numerous weaker events were captured. From these events it occurs that aerosol mass, total water and pH are mostly driven by the coarse aerosol fraction. This is consistent with the findings of Koulouri et al. (2008) that most (86%) of the mass of crustal components were found in coarse particles. In terms of mass concentration, the two natural sources, namely air masses of marine and dust origin, contain the largest amounts of total submicron water. Even though total water exhibits the highest mass concentrations for the specific sources, the relative

contribution of organic water to the submicron fraction is the lowest (16% for dust and 17% for marine, based on the median values). For the two natural sources, the ratio between submicron pH and calculated pH for the PM_{10} fraction is the lowest observed (Table 1), namely 30±17% (median 25%) and 6±19% (median 5%).

3.5 Atmospheric implications

The pH values for submicron and PM_{10} fractions is also expected to affect many processes, such as the solubility and therefore the bioavailability of nutrients and especially phosphorus (P) and iron (Fe). This is of crucial importance for seas such as the eastern Mediterranean for which primary productivity is P limited (Krom et al., 1991). One of the striking results of the aerosol pH calculations (presented in Table 1) is that with the exception of biomass burning, pH of all submicronic aerosols including those originating from desert dust is highly acidic with values typically below 2. Although the nutrient flux from the fine mode is certainly smaller than in the coarse mode, it can be transported much further away from source regions before deposition, and be considerably more acidified (hence bioavailable). Based on published literature (Nenes et al., 2011; Meskhidze et al., 2003) under acidic conditions similar to the derived pH aerosol values, the acid-mobilized dissolution of such nutrients is expected to be of great importance.

Markaki et al. (2003), by analyzing PM_{10} aerosols collected in Greece (Finokalia) and Turkey (Erdemli) for dissolved inorganic (DIP) and Total (TP) phosphorus levels have shown that although the SW sector, corresponding to the Sahara, presented TIP levels by a factor of two higher than the European (NE or NW) sectors, the lowest values for the DIP/TIP ratio are associated with the SE and SW sectors, and the highest with the N sectors (difference of almost a factor of 2). The explanation for that behavior is given by the ratio of pH in PM_1 and PM_{10} aerosols that is presented in Table 1. In aerosols from the NW sector only a very small difference in pH between the two fractions is observed, while in desert aerosols the large amount of dust present in the coarse mode highly influences pH of PM_{10} leading to a significant decrease of acidity and thus P solubility. However as dust events can transport large amounts of P (up to a factor of three higher than in air masses coming from Europe), any future change in PM_1/PM_{10} ratio caused by dust events will significantly influence P availability and deposition to the eastern Mediterranean sea and thus to its productivity.

Conclusion

Using the aerosol chemical composition measurements by ACSM, thermodynamic models, such as ISORROPIA-II, and CCN measurements we calculated the particle water associated with both inorganics (W_{inorg}) and organics (W_{org}) aerosol components. The sum of these two (W_{inorg}+W_{org}) equal to the total particle water is then compared to the LWC determined by the two nephelometers operating in dry and wet mode, respectively. Predicted aerosol water was compared to LWC determined from ambient versus dry light scattering coefficients. At Finokalia the sum of W_{inorg} and W_{org} was highly correlated and in close agreement with the measured LWC (on average within 10%), with slope=0.92 and R^2=0.8 for the whole measurement period (n=5201 points). As expected, the highest fine aerosol water values are observed during nighttime, when RH is also at its maximum, resulting in significant water uptake. W_{org} shows a significant diurnal variability with morning and afternoon average mass concentrations being 10-15 times lower than nighttime concentrations. Thus, during daytime W_{inorg} is the main form of particle water as the average values for the predicted water (W_{org}+W_{inorg}) are very close to the ones of the inorganic water alone. On the other hand, during nighttime, the contribution of organic water to the total aerosol water increases becoming significant during nighttime, when the photochemical activity and temperature are minimum. The average concentration of total aerosol water was found to be 2.19±1.75 μg m^{-3}, which according to the dry mass measurements, can contribute on average up to 33% of the total submicron mass concentration. The average aerosol water associated with organics, W_{org}, was found to be 0.56±0.37 μg m^{-3}, which constitutes about 27.5% of the total calculated water. The overall uncertainty of this calculation is estimated to be around 30%.

Based on aerosol water, particle pH is also calculated, a parameter which is very important for the atmospheric implications of aerosols but is difficult to measure directly. In the eastern Mediterranean during the studied period, aerosol pH varied from 0.5 to 2.8 indicating that the aerosol was highly acidic throughout the period. Biomass burning aerosol presented the highest values of pH in the submicron fraction and the lowest values in total water mass concentration. Interestingly enough, the value of 2.8 for biomass burning pH is well above the value of 2, which is a lower limit for the occurrence of nitrate's condensation. The correlation, which has been observed during fire events between biomass burning organic aerosol and particulate nitrates, may be explained by these pH levels, which favor nitrate condensation. It can be seen that, in general, for anthropogenic-laden air masses (e.g. from Istanbul, Black Sea and Continental Europe) aerosol

mass resides mainly in the submicron aerosol (60-70%) and thus the submicron fraction seems also to drive the pH of PM_{10}, while most of the aerosol water (~70%) is present in the coarse fraction. pH is driven by the fine mode while on the contrary, the grand majority of the aerosol water is present in the coarse mode. This may be due to the important contributions of the hygroscopic sea salt components in the coarse mode and of the less hygroscopic organics in the fine mode.

In terms of mass concentration, the air masses affected by the two natural sources, namely of marine and dust origin, contain the largest amounts of total submicron water. Even though total water exhibits the highest mass concentrations for the specific sources, the relative contribution of organic water to the submicron fraction is the lowest (~19% for dust and ~15.5% for marine). For these two natural sources, the ratio between submicron pH and calculated pH for the PM_{10} fraction is the lowest observed, 30±17% (median 25%) and 6±19% (median 5%).

The low pH values observed during the studied period in the submicron mode and independently of air masses origin could have significant implications for nutrient availability and especially for P solubility which is the nutrient limiting sea water productivity of the eastern Mediterranean.

Acknowledgments. This research has been co-financed by the European Union (European Social Fund – ESF) and Greek national funds through the Operational Program "Education and Lifelong Learning" of the National Strategic Reference Framework (NSRF) - Research Funding Program ARISTEIA I - PANOPLY. The authors gratefully acknowledge the NOAA Air Resources Laboratory (ARL) for the provision of the HYSPLIT transport and dispersion model and READY website (http://www.ready.noaa.gov) used in this publication.

References

APHA, AWWA, WEF, (2000) Standard Methods for the Examination of Water and Wastewater, 20th ed. American Public Health Association, Washington DC.

Bougiatioti, A., Zarmpas, P., Koulouri, E., Antoniou, M., Theodosi, C., Kouvarakis G., Saarikoski, S., Mäkelä, T., Hillamo, R., and Mihalopoulos, N.: Organic, elemental and water-soluble organic carbon in size segregated aerosols, in the marine boundary layer of the Eastern Mediterranean, Atmos. Environ., 64, 251-262, 2013.

Bougiatioti A., Stavroulas, I., Kostenidou, E., Zarmpas, P., Theodosi, C., Kouvarakis, G., Canonaco, F., Prévôt, A.S.H., Nenes, A., Pandis, S.N., and Mihalopoulos, N.: Processing of biomass-burning aerosol in the easter Mediterranean during summertime, Atmos. Chem. Phys., 14, 4793-4807, doi:10.5194/acp-14-4793-2014, 2014.

Bougiatioti, A., Bezantakos, S., Stavroulas, I., Kalivitis, N., Kokkalis, P., Biskos, G., Mihalopoulos, N., Papayannis, A., and Nenes, A.: Influence of biomass burning on CCN number and hygroscopicity during summertime in the eastern Mediterranean, Atmos. Chem. Phys. Discuss., 15, 21539-21582, doi:10.5194acpd-15-21539-2015, 2015.

Carlton, A. G. and Turpin, B. J.: Particle partitioning potential of organic compounds is highest in the Eastern US and driven by anthropogenic water, Atmos. Chem. Phys., 13, 10203–10214, doi:10.5194/acp-13-10203-2013, 2013.

Cerully, K. M., Bougiatioti, A., Hite Jr., J. R., Guo, H., Xu, L., Ng, N. L., Weber, R., and Nenes, A.: On the link between hygroscopicity, volatility, and oxidation state of ambient and water-soluble aerosol in the Southeastern United States, Atmos. Chem. Phys. Discuss., 14, 30835-30877, doi:10.5194/acpd-14-30835-2014, 2014.

Eddingsaas, N. C., VanderVelde, D. G., and Wennberg, P. O.: Kinetics and Products of the Acid-Catalyzed Ring-Opening of Atmospherically Relevant Butyl Epoxy Alcohols, J. Phys. Chem. A, 114, 8106–8113, doi:10.1021/Jp103907c, 2010.

Fountoukis, C., and Nenes, A.: ISORROPIA II: a computationally efficient thermodynamic equilibrium model for K^+-Ca^{2+}-Mg^{2+}-NH_4^+-Na^+-SO_4^{2-}-NO_3^--Cl^--H_2O aerosols, Atmospheric Chemistry and Physics, 7, 4639-4659, 2007.

Fountoukis, C., Nenes, A., Sullivan, A., Weber, R., Van Reken, T., Fischer, M., Matias, E., Moya, M., Farmer, D., and Cohen, R. C.: Thermodynamic characterization of Mexico City aerosol during MILAGRO 2006, Atmospheric Chemistry and Physics, 9, 2141-2156, 2009.

Guo, H., Xu, L., Bougiatioti, A., Cerully, K.M., Capps, S.L., Hite, J.R., Carlton, A.G., Lee, S.-H., Bergin, M.H., Ng, N.L., Nenes, A., and Weber, R.J.: Particle water and pH in the southeastern United States, Atmospheric Chemistry and Physics, 15, 5211-5228, doi:10.5194/acp-15-5211-2015, 2015.

Hennigan, C. J., Izumi, J., Sullivan, A. P., Weber, R. J., and Nenes, A.: A critical evaluation of proxy methods used to estimate the acidity of atmospheric particles, Atmos. Chem. Phys., 15, 2775– 2790, doi:10.5194/acp-15-2775-2015, 2015.

Jickells, T.D., Z. S. An, K. K. Andersen, A. R. Baker, G. Bergametti, N. Brooks, J. J. Cao, P. W. Boyd, R. A. Duce, K. A. Hunter, et al., Global iron connections between desert dust, ocean biogeochemistry, and climate. Science 308:67–71, 2005.

Keene, W. C., A. A. P. Pszenny, J. R. Maben, and R. Sander: Variation of marine aerosol acidity with particle size, Geophys. Res. Lett., 29(7), doi:10.1029/2001GL013881, 2002.

Keene, W.C., Pszenny, A.A.P., Maben, J.R., Stevenson, E., Wall, A.: Closure evaluation of size-resolved aerosol pH in the New England coastal atmosphere during summer, J. Geophys. Res., 109, D23307, doi:10.1029/2004JD004801, 2004.

Khlystov, A., Stanier, C.O., Takahama, S. and Pandis, S.N.: Water content of ambient aerosol during the Pittsburgh Air Quality Study, J. Geophys. Res. Atmospheres, Vol 110, Issue D7, doi:10.1029/2004JD004651, 2005.

Kim, J., Yoon, S.-C., Jefferson, A., and Kim, S.-W.: Aerosol hygroscopic properties during Asian dust, pollution, and biomass burning episodes at Gosan, Korea in April 2001, Atmospheric 635 Environment, 40, 1550-1560, 10.1016/j.atmosenv.2005.10.044, 2006.

Koulouri, E., Saarikoski, S., Theodosi, C., Markaki, Z., Gerasopoulos, E., Kouvarakis, G., Mäkelä, T., Hillamo, R., and Mihalopoulos, N.: Chemical composition and sources of fine and coarse aerosol particles in the Eastern Mediterranean, Atmos. Environ., 42, 6542-9550, 2008.

Kouvarakis, G. Mihalopoulos, N., Tselepides, T., Stavrakakis, S.: On the importance of atmospheric nitrogen inputs on the productivity of Easter Mediterranean, Global Biochem. Cycles, 15, 805-818, 2001.

Kreidenweis, S. M., Petters, M. D., and DeMott, P. J.: Singleparameter estimates of aerosol water content, Environ. Res. Lett., 3, 035002, doi:10.1088/1748-9326/3/3/035002, 2008.

Krishnamurthy, A., Moore, J.K., Mahowald, N., Luo, C., and Zender, C.S.: Impacts of atmospheric nutrient inputs on marine biogeochemistry, J. Geophys. Res., 115, G01006, doi:10.1029/2009JG001115, 2010.

Krom, M.D., Kress, N., Brenner, S., and Gordon, L.I.: Phosphorus limitation of primary productivity in the eastern Mediterranean Sea, Limnol. Oceanogr., 36 (3), 424-432, 1991.

Lee, T., Sullivan, A. P., Mack, L., Jimenez, J. L., Kreidenweis, S. M., Onasch, T. B., Worsnop, D. R., Malm, W., Wold, C. E., Hao, W. M., and Collett, J. L.: Variation of chemical smoke marker emissions during flaming vs. smoldering phases of laboratory open burning of wildland fuels, *Aerosol Sci. Technol.*, **44**, 1–5, doi:10.1080/02786826.2010.499884, 2010.

Liao, H. and Seinfeld, J. H.: Global impacts of gas-phase chemistry aerosol interactions on direct radiative forcing by anthropogenic aerosols and ozone, J. Geophys. Res.-Atmos., 110, D18208, doi:10.1029/2005jd005907, 2005.

Magi, B. I.: Effects of humidity on aerosols in southern Africa during the biomass burning season, Journal of Geophysical Research, 108, doi:10.1029/2002jd002144, 2003.

Mahowald, N., Jickells, T.D., Baker, A.R., Artaxo, P., Benitez-Nelson, C.R., Bergametti, J., Bond, T.C., Chen, Y., Cohen, D.D., Herut, B., Kubilay, N., Losno, R., Luo, C., Maenhaut, W., McGee, K.A., Okin, G.S., Siefert, R.L., and Tsukuda, S.: Global distribution of atmospheric phosphorus sources, concentrations and deposition rates, and anthropogenic impacts, Global Biogeochem. Cycles, 22, GB4026, doi:10.1029/2008GB003240, 2008.

Mahowald, N. M., Engelstaedter, S., Luo, C., Sealy, A., Artaxo, P., Benitez-Nelson, C., Bonnet, S., Chen, Y., Chuang, P.Y., Cohen, D.D., Dulac, F., Herut, B., Johansen, A.M., Kubilay, N., Losno, R., Maenhaut, W., Paytan, A., Prospero, J.M., Shank, L.M., and Siefert, R.L.: Atmospheric iron deposition: Global distribution, variability, and human perturbations, Annu. Rev. Mater. Sci., 1, 245–278, doi:10.1146/annurev.marine.010908.163727, 2009.

Meskhidze, N., Chameides, W.L., Nenes, A., and Chen, G.: Iron mobilization in mineral dust: Can anthropogenic SO_2 emissions affect ocean productivity?, *Geophys. Res. Let.*, 30 (21), doi:10.1029/2003GL018035, 2003.

Meskhidze, N, Chameides, W. and Nenes, A. (2005) Dust and Pollution: A Recipe for Enhanced Ocean Fertilization? *J.Geoph.Res.*,**110**, D03301, doi:10.1029/2004JD005082

Mihalopoulos, N., Stephanou, E., Kanakidou,M., Pilitsidis, S., and Bousquet, P.: Troposheric aerosol ionic composition above the eastern Mediterranean area, *Tellus B*, **49**, 314–326, 1997.Moore, R.H., and Nenes, A.: Scanning Flow CCN Analysis-A method for fast measurements of CCN spectra, Aerosol Sci. Technol., 43:12, 1992-1207, 2009.

Myriokefalitakis, S., Tsigaridis, K., Mihalopoulos, N., Sciare, J., Nenes, A., Kawamura, K., Segers, A., and Kanakidou, M.: In-cloud oxalate formation in the global troposphere: a 3-D modeling study, Atmos. Chem. Phys., 11, 5761–5782, doi:10.5194/acp-11-5761-2011, 2011.

Myriokefalitakis, S., Daskalakis, N., Mihalopoulos, N., Baker, A. R., Nenes, A., and Kanakidou, M.: Changes in dissolved iron deposition to the oceans driven by human activity: a 3-D global modelling study, Biogeosciences, 12, 3973-3992, doi:10.5194/bg-12-3973-2015, 2015.Nenes, A., Krom, M. D., Mihalopoulos, N., Van Cappellen, P., Shi, Z., Bougiatioti, A., Zarmpas, P., and Herut, B.: Atmospheric acidification of mineral aerosols: a source of bioavailable phosphorus for the oceans, Atmos. Chem. Phys., 11, 6265–6272, doi:10.5194/acp-11-6265-2011, 2011.

Ng, N.L., Herndon, S.C., Trimborn, A., Canagaratna, M.R., Croteau, P.L., Onasch, T.B., Sueper, D., Worsnop, D.R., Zhang, Q., Sun, Y.L., and Jayne, J.T.: An Aerosol Chemical Speciation Monitor (ACSM) for routine monitoring of the composition and mass concentration of ambient aerosol., *Aerosol Sci. Technol.*, **45** (7), 780-794, 2011.

Nguyen, T.K.V., Petters, M.D., Suda, S.R., Guo, H., Weber, R.J., and Carlton, A.G.: Trends in particle-phase liquid water during the Southern Oxidant and Aerosol Study, Atmos. Chem. Phys., 14, 10911-10930, doi:10.5194/acp-14-10911-2014, 2014.

Nowak, J. B., Huey, L. G., Russell, A. G., Tian, D., Neuman, J. A., Orsini, D., Sjostedt, S. J., Sullivan, A.P., Tanner, D. J., Weber, R. J., Nenes, A., Edgerton, E., and Fehsenfeld, F. C.: Analysis of urban gas phase ammonia measurements from the 2002 Atlanta Aerosol Nucleation and Real-Time Characterization Experiment (ANARChE), Journal of Geophysical Research, 111, 10.1029/2006jd007113, 2006.

Petters, M.D., and Kreidenweis, S.M.: A single parameter representation of hygroscopic growth and cloud condensation nucleus activity, *Atmos. Chem. Phys.*, 7, 1961-1971, doi: 10.5194/acp-8-6273-2008, 2007.

690 Pilinis, C., Pandis, S. N., and Seinfeld, J. H.: Sensitivity of Direct Climate Forcing by Atmospheric
691 Aerosols to Aerosol-Size and Composition, J. Geophys. Res.-Atmos., 100, 18739–18754,
692 doi:10.1029/95jd02119, 1995.
693 Pöschl, U., and Shiraiwa, M.: Multiphase chemistry at the atmosphere-biosphere interface
694 influencing climate and public health in the Anthropocene, Chem. Rev., 115, 4440-4475,
695 doi:10.2021/cr500487s, 2015
696 Roberts, G.C., and Nenes, A.: A continuous-flow streamwise thermal-gradient CCN chamber for
697 atmospheric measurements, *Aerosol Sci. Technol.*, 39, 206-221,
698 dpo:10.1080/027868290913988, 2005.
699 Sheridan, P. J.: Spatial variability of submicrometer aerosol radiative properties over the Indian
700 Ocean during INDOEX, Journal of Geophysical Research, 107, 10.1029/2000jd000166, 2002.
701 Shi, Z., Krom, M.D., Jickells T.D., Bonneville, S., Carslaw, K.S., Mihalopoulos, N., Baker, A.R.,
702 Benning, L.G.: Impacts on iron solubility in the mineral dust by processes in the source region
703 and the atmosphere: A review, Aeol. Res. 5, 21–42, doi:/10.1016/ j.aeolia.2012.03.001, 2012.
704 Solmon, F., Chuang, P.Y., Meskhidze, N., and Chen, Y.: Acidic processing of mineral dust iron
705 by anthropogenic compounds over the north Pacific Ocean, J. Geophys. Res., Atmospheres,
706 114 (D2), doi:10.1029/2008JD010417, 2009.
707 Spindler, G., Hesper, J., Brüggemann, E., Dubois R., Müller, Th., and Herrmann, H.: Wet annular
708 denuder measurements of nitrous acid: laboratory study of the artefact reaction of NO_2 with
709 S(IV) in aqueous solution and comparison with field measurements, Atmos. Environ., 37, 2643-
710 2662, 2003.
711 A. F. Stein, R. R. Draxler, G. D. Rolph, B. J. B. Stunder, M. D. Cohen, and F. Ngan, 2015: NOAA's
712 HYSPLIT Atmospheric Transport and Dispersion Modeling System. *Bull. Amer. Meteor.*
713 *Soc.*, **96**, 2059–2077, doi: http://dx.doi.org/10.1175/BAMS-D-14-00110.1, 2015.
714 Stookey, L. C.: Ferrozine - a new spectrophotometric reagent for iron. Analytical Chemistry 42,
715 779–781, 1970.
716 Stumm, W. and Morgan, J. J.: Aquatic Chemistry, Wiley- Interscience, New York, 1996.
717 Surratt, J. D., Lewandowski, M., Offenberg, J. H., Jaoui, M., Kleindienst, T. E., Edney, E. O., and
718 Seinfeld, J. H.: Effect of acidity on secondary organic aerosol formation from isoprene, Environ.
719 Sci. Technol., 41, 5363–5369, doi:10.1021/es0704176, 2007.

720 Surratt, J. D., Chan, A. W., Eddingsaas, N. C., Chan, M., Loza, C. L., Kwan, A. J., Hersey, S. P.,
721 Flagan, R. C.,Wennberg, P. O., and Seinfeld, J. H.: Reactive intermediates revealed in secondary
722 organic aerosol formation from isoprene, P. Natl. Acad. Sci. USA, 107, 6640–6645,
723 doi:10.1073/pnas.0911114107, 2010.
724 Weber, R.J., Guo, H., Russel, A.G., and Nenes, A.: High aerosol acidity despite declining
725 atmospheric sulfate concentrations over the past 15 years, Nat. Geosci., *in press*, 2016.
726 Wyers, G.P., Otjes, R.P., Slanina, J.: A continuous-flow denuder for the measurement of ambient
727 concentrations and surface-exchange fluxes of ammonia, Atmos. Environ., 27, 2085–2090,
728 1993.
729 Zhang, Z., Gao, J., Engling, G., Tao, J., Chai, F., Zhang, L., Zhang, R., Sang, X., Chan, C., Lin,
730 Z., and Cao, J.: Characteristics and applications of size-segregated biomass burning tracers in
731 China's Pearl River Delta region, Atmos. Environ., 102, 290-301, 2015.

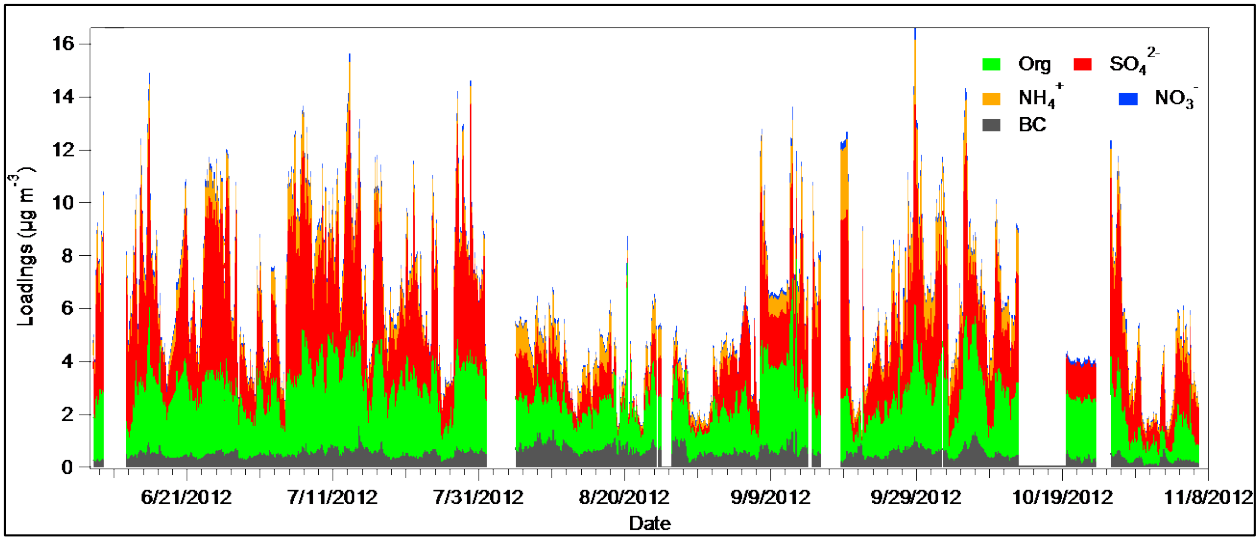

Figure 1: Time series of the main submicron aerosol components at Finokalia, Crete, during the measurement period in 2012.

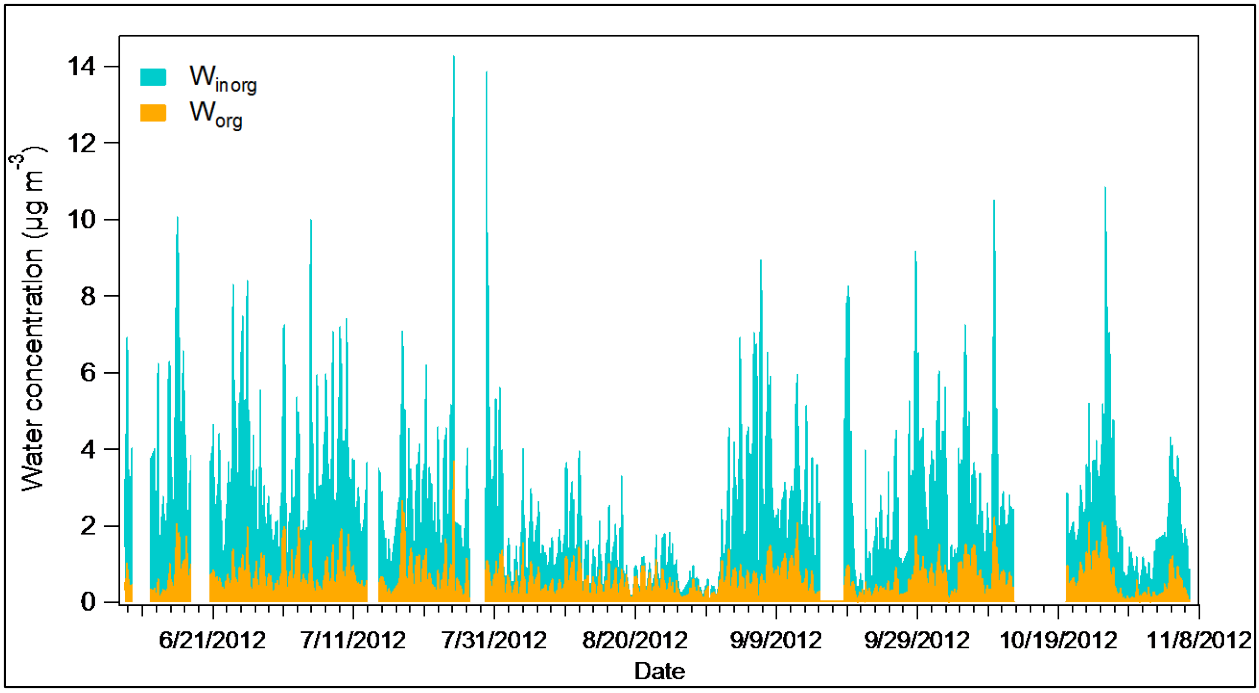

736

737 **Figure 2:** Time series of the two calculated aerosol water components, the water associated with

738 the inorganic (W_{inorg}) and the organic (W_{org}) aerosol components.

739

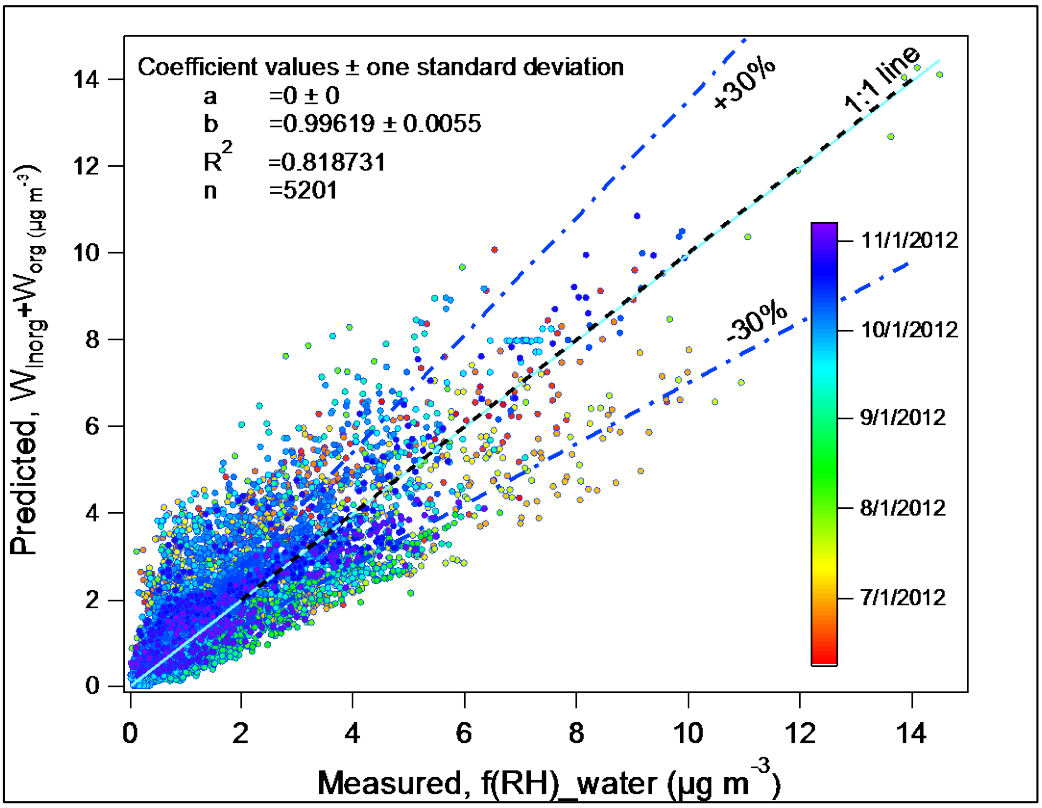

Figure 3: Correlation between calculated and measured LWC of aerosol.

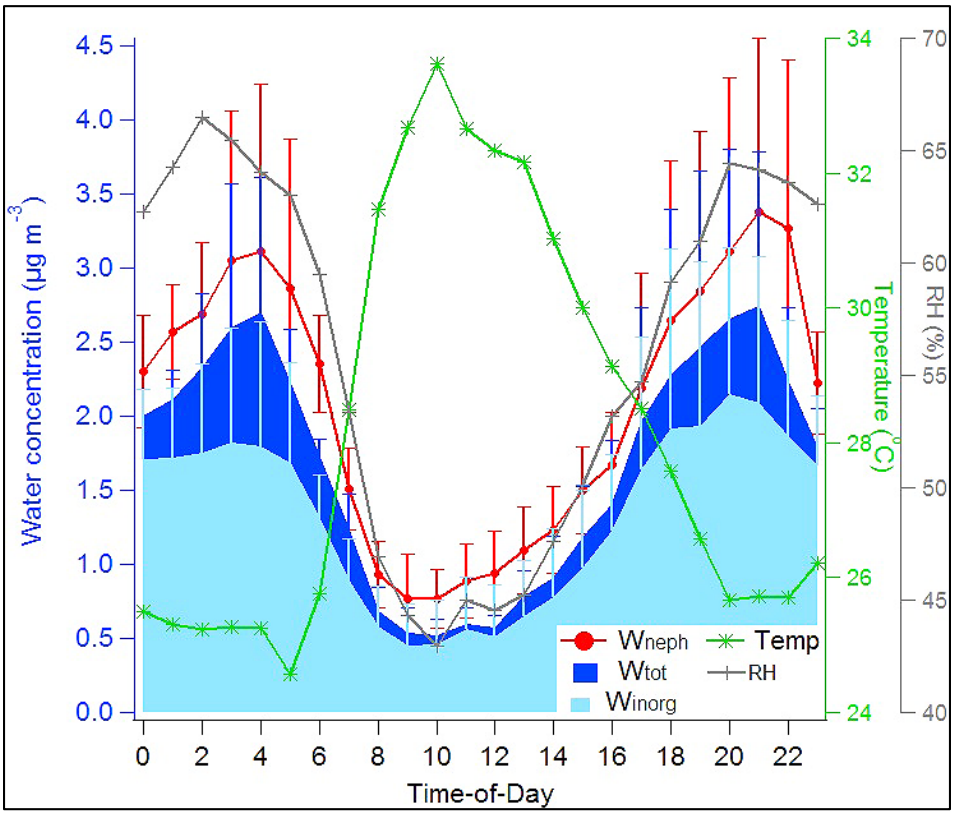

Figure 4: Diurnal profiles of predicted and measured water, along with measured RH and T. Average hourly averages and standard deviations plotted as error bars in local hour are shown.

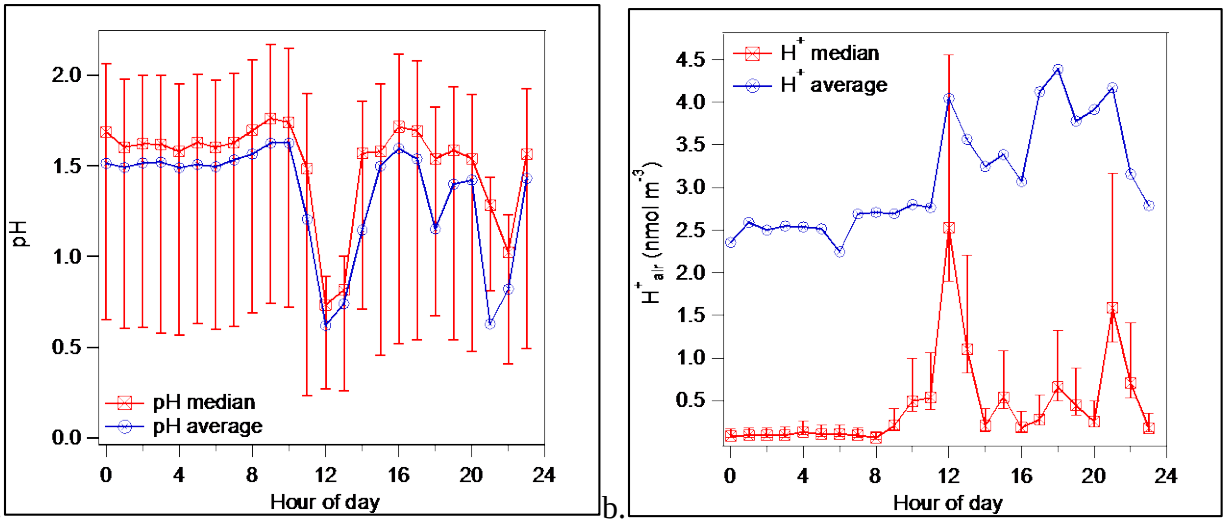

a. b.

Figure 5: Diurnal profile of pH (a) and H^+ (b) calculated based on total predicted water and hydronium concentrations predicted by ISORROPIA-II. Average and median (with 25%, 75% quantiles) values are provided.

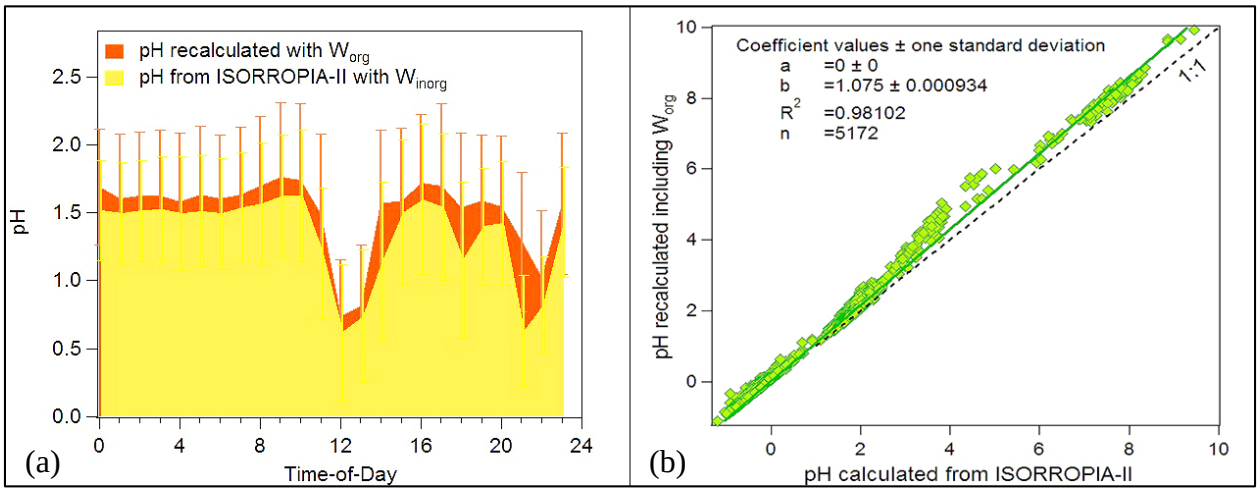

Figure 6: a) Diurnal variability of pH based on total predicted water (orange using both W_{org} and W_{inorg}) and only the inorganic water (yellow using only W_{inorg}), respectively. Average hourly values and standard deviation in the form of error bars are provided, b) Comparison between the pH predicted by ISORROPIA-II based on inorganic aerosol composition and that recalculated including also the organic component.

776 **Table 1**: Average values of water content (total and organic) and pH with standard deviation and
777 median values in parenthesis.
778

	PM_1			PM_1/PM_{10}		
Source / region	**$water_{tot}$ ($\mu g\ m^{-3}$)**	**$water_{org}$ ($\mu g\ m^{-3}$)**	**pH**	**mass**	**$water_{tot}$**	**pH**
Biomass Burning (n=7)	1.33±1.22 (1.56)	0.37±0.33 (0.39)	2.77±0.88 (2.67)	0.48±0.16 (0.47)	0.08±0.09 (0.05)	0.89±0.2 (0.93)
Istanbul & Black Sea (n=7)	1.72±0.54 (1.21)	0.81±0.34 (0.75)	1.92±0.24 (2.00)	0.72±0.09 (0.69)	0.33±0.21 (0.26)	0.94±0.67 (0.88)
Continental Europe (n=9)	1.52±0.64 (1.32)	0.48±0.34 (0.47)	1.30±0.19 (1.26)	0.60±0.18 (0.64)	0.31±0.17 (0.28)	0.58±0.47 (0.50)
Dust (n=7)	2.48±0.54 (2.44)	0.48±0.22 (0.39)	1.48±0.44 (1.59)	0.34±0.08 (0.38)	0.39±0.08 (0.29)	0.30±0.17 (0.25)
Marine (n=7)	2.38±1.24 (1.91)	0.37±0.17 (0.34)	0.44±0.67 (0.43)	0.58±0.27 (0.57)	0.83±0.6 (0.70)	0.06±0.19 (0.05)

779